Water SA 51(3) 181–190 / Jul 2025
https://doi.org/10.17159/wsa/2025.v51.i3.4190

Research paper

Evaluation of Sentinel-2 for water quality monitoring in a eutrophic estuary in South Africa

Marié E Smith[1,2], Daniel A Lemley[3,4], Emily Whitfield[3,4] and Janine B Adams[3,4]

[1]*Coastal Systems and Earth Observation Research Group, Council for Scientific and Industrial Research (CSIR), Rosebank 7700, Cape Town, South Africa*
[2]*Department of Oceanography, University of Cape Town, Rondebosch 7700, Cape Town, South Africa*
[3]*Botany Department, Nelson Mandela University, Gqeberha 6031, South Africa*
[4]*DSI/NRF Research Chair in Shallow Water Ecosystems and the Institute for Coastal and Marine Research, Gqeberha 6031, South Africa*

This study evaluates the utility of Sentinel-2 satellite products for monitoring spatial and temporal changes in chlorophyll *a* (Chl-*a*) concentration within an urban, eutrophic estuary. Four atmospheric correction (AC) processors, namely Acolite, C2RCC, Sen2Cor, and Polymer, are assessed together with eight different parameterisations of three high-biomass-appropriate empirical Chl-*a* retrieval algorithms, namely the 2-band, 3-band and normalised difference chlorophyll index (NDCI). The best performance is achieved using Sen2Cor and the NDCI, which provides an average absolute percentage difference, bias, and correlation of 173%, 23.8% and 0.853 ($p < 0.05$), respectively, which improves to 61.7%, 5.4% and 0.843 ($p < 0.05$), respectively, for conditions where Chl-*a* > 10 mg/m^3. These results indicate that an appropriately configured NDCI algorithm applied to the default Sentinel-2 Level 2 product can be used for routine aquatic water quality monitoring applications for mesotrophic and eutrophic estuaries in the South African context. Monitoring approaches for estuary water quality are essential, as there is an increase in urban runoff and untreated inputs from malfunctioning wastewater treatment systems. The results inform water quality monitoring and management of similar sized estuaries globally. Remote sensing can complement *in situ* measurements and provide a holistic overview of a system.

CORRESPONDENCE
Marié E Smith

EMAIL
Msmith2@csir.co.za

DATES
Received: 17 January 2025
Accepted: 7 June 2025

KEYWORDS
Sentinel-2
water quality
chlorophyll *a*
atmospheric correction
South Africa

INTRODUCTION

Chlorophyll *a* (Chl-*a*) concentration is often used as a proxy for phytoplankton biomass and serves as an indicator for estuarine eutrophication that occurs as a consequence of anthropogenic nutrient enrichment (Lemley et al., 2015). *In situ* monitoring can be expensive, time-consuming, and under-representative of an entire water body's geographic extent or temporal changes. Satellite-derived data products provide a routine, inexpensive means to assess a system's spatial and temporal scales of variability. Remote sensing has some known limitations regarding the information it can retrieve, such as being limited to the surface layers of a water body, being impacted by cloud cover, and only being capable of retrieving some water quality indicators (IOCCG, 2018); as such it is not meant to replace *in situ* measurements, but can offer complementary information that provides a more holistic overview of a system.

Operational satellite-based products are routinely provided over the coastal marine environment through the South African National Ocean and Coastal Information Management System (OCIMS; Krug et al., 2024); however, these moderate spatial resolution products (300 m) do not have appropriately high spatial resolution to resolve the fine-scale variability within almost all of South Africa's estuaries. The Operational Land Imager (OLI) on board Landsat-8 and the Multi-Spectral Instrument (MSI) on board the Sentinel-2 constellation both offer appropriate spatial resolutions and can provide science-quality products over coastal and inland waters (Ansper and Alikas, 2018; Franz et al., 2015; Llodrà-Llabrés et al., 2023; Vanhellemont and Ruddick, 2015). While Landsat-8 only has a 16-day revisit time and 30 m spatial resolution, Sentinel-2 has a 5-day revisit time and 10–60 m spatial resolution, with the addition of a 705 nm band which is particularly useful for deriving Chl-*a* concentrations in inland, eutrophic, or optically complex waters (Moses et al., 2009). Although MSI was designed for land applications, it has sufficient spectral and radiometric performance to facilitate remote sensing of smaller aquatic targets (Pahlevan et al., 2017). Many studies have used Sentinel-2 to detect water column Chl-*a* concentration (Llodrà-Llabrés et al., 2023, and references therein). However, it has not been widely used to monitor Chl-*a* in water bodies under 1 km^2 in size. Bangira et al. (2023) showed that, at the time of publication, there had been only 8 studies (in English, in peer-reviewed journals accredited by the South African Department of Higher Education and Training) that used Sentinel-2 data for case studies estimating water quality indicators in African reservoirs, of which only two represented estimations of Chl-*a*. Only two peer-reviewed studies have assessed Sentinel-2 performance for monitoring Chl-*a* in South African reservoirs (Obaid et al., 2021; Ndou, 2023). However, none have considered estuarine environments or different atmospheric correction methods. The current study aims to assess the performance of a selection of established, freely available atmospheric correction methods for Sentinel-2, in combination with several published Chl-*a* algorithms, in a small, eutrophic estuary. The results will inform the potential and limitations of operational remotely sensed water quality management in the Swartkops Estuary, and similar environments.

METHODOLOGY

Sampling site and *in situ* measurements

The Swartkops Estuary is a predominantly open low-inflow estuary located on the warm temperate south coast of South Africa. The estuary is highly urbanised and susceptible to eutrophic conditions due to excessive nutrient inputs from adjacent stormwater outlets (Lemley et al., 2022; Mmachaka et al., 2023) and upstream wastewater treatment works (Lemley et al., 2023). Similarly, the augmented nature of these nutrient-rich baseflows has reduced hydrological variability in the middle to upper reaches of the estuary and facilitated the accumulation of high-biomass phytoplankton blooms in these areas (Adams et al., 2025). This study focuses on estuarine spatial survey data collected from April 2019 to October 2021, covering austral seasonal variability and HAB events. Surface water samples were collected at 6 fixed stations, as shown in Fig. 1, and phytoplankton biomass (measured as Chl-*a* concentration) was determined spectrophotometrically according to the methods of Nusch (1980). The Chl-*a* concentration ranged from 0.5 to 744.8 mg/m^3 during the study period (Lemley et al., 2023). Samples were taken within the centre of the main channel, approximately 50 and 20 m from shore at Stations 1–5 and 6, respectively. The optical depth varied between sampling dates within the range of 0.3 to 2.2 m, but it was always highest near the mouth and declined upstream.

Satellite data: Matchup and data extraction procedure

Level-1C data for Tile T35HLC from Sentinel-2 MSI were obtained from the Copernicus Open Access Hub (2023). Only satellite data from valid water pixels were considered for matchups, with reflectance > 0, ±3 hours from an *in situ* measurement. Satellite estimates were extracted over a 3 x 3 pixel box, equivalent to 30 x 30 m, centred over the matchup station, but were only used if consisting of >4 valid pixels. A glint mask was applied to the Sen2Cor data by discarding all data where the reflectance at the 1 610 nm band was greater than 0.05. The 9 different dates and times that coincided with Sentinel-2 satellite overpasses are shown in Table 1.

Additional processing and time-series analyses of Sentinel-2 Level-2A data were performed using the Digital Earth Africa (2024) Analysis Sandbox. The Digital Earth Africa Analysis Sandbox is a free Cloud-based platform that operates using a Jupyter Lab environment, allowing access to analysis-ready datasets covering all of Africa.

Satellite data: atmospheric correction

This study compared the outputs of 4 different atmospheric correction (AC) procedures. The atmospheric correction for OLI 'lite' (Acolite; v.20221114) (Vanhellemont and Ruddick, 2018) is an image-based AC model for use over inland and coastal waters. The dark spectrum fitting (DSF) approach (Vanhellemont, 2019) was applied using the default settings without the mask for negative water-leaving reflectance.

The Case 2 Regional CoastColour (C2RCC; v1.2) per-pixel artificial neural network inversion (Brockmann et al., 2016) was applied using the Sentinel Application Platform (SNAP v.9.0) graph processing tool with default settings.

Table 1. Date and time (UTC) of Sentinel-2 overpasses, which coincided with *in situ* matchup data

Number	Date	Time: Sentinel-2A	Time: Sentinel-2B
1	25 April 2019	07:56:11	
2	4 February 2020		08:00:29
3	24 February 2020		07:59:19
4	2 March 2020		07:48:29
5	5 March 2020		07:58:09
6	5 June 2020	07:46:21	
7	25 June 2020	07:46:21	
8	12 November 2020	07:51:51	
9	26 January 2021		07:51:09

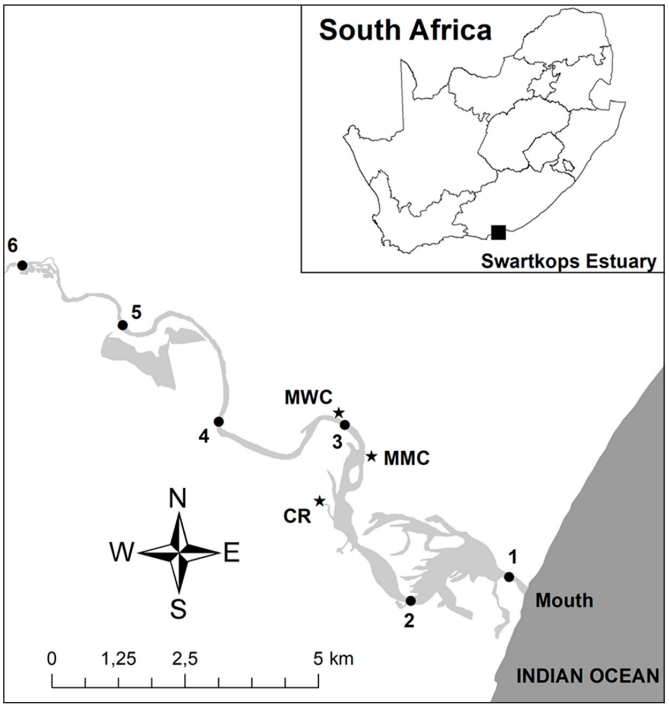

Figure 1. Locations of the 6 sampling stations on the Swartkops Estuary in relation to point sources of nutrient inputs from the Chatty River (CR), Markman Canal (MMC), and Motherwell Canal (MWC) (adapted from Lemley et al., 2023, Fig. 1)

The polynomial-based algorithm applied to MERIS (Polymer; v4.13) (Steinmetz et al., 2011; Steinmetz and Ramon, 2018) is a physical model that uses a spectral matching method based on a polynomial to model the spectral reflectance of the atmosphere and sunglint, a water reflectance model, and utilises all visible spectral bands in the correction.

Sentinel-2 Correction (Sen2Cor; v.2.11) (Main-Knorn et al., 2017; Müller-Wilm et al., 2018) is the default AC for the Sentinel-2 Level-2A land product. The approach requires the presence of dark, dense vegetation, water or dark soil pixels in an image to be used as a reference (Kaufman et al., 1997). It operates on the assumption that the ratios between the bottom of the atmosphere reflectances at different wavelengths (490 and 665 to 2 190 nm) are constant.

All outputs were either automatically provided at, or resampled to, 10 m spatial resolution. Where the AC output was not provided automatically as R_{rs}, the output reflectance was divided by pi. To facilitate the operational application of water quality monitoring, this study focused on efficient and freely available AC algorithms that do not require human or external input and can be easily incorporated into computational processing chains; in this study, all algorithms were operated using Python 3.9.

Chl-*a* algorithms

The Swartkops Estuary provides an ideal case study to test the efficacy of Sentinel-2 processing algorithms for monitoring Chl-*a* concentrations in small complex estuaries, due to its eutrophic nature. The severity of eutrophic symptoms in the system is evidenced by near-year-round accumulations of high-biomass phytoplankton blooms (>60 mg/m^3) in the high-retention middle to upper reaches (Adams et al., 2019; Lemley et al., 2023). As such, we focused on the assessment of algorithms with previous success in high-biomass optically complex environments operating in the red, red-edge, and NIR spectral regions. We evaluated the performance of three of the most well-established Chl-*a* retrieval indices for Sentinel-2 (Llodrà-Llabrés et al., 2023), including the 2-band (2B) (Gitelson and Kondratyev, 1991) and 3-band (3B) algorithms (Dall'Olmo et al., 2003), and the normalised difference chlorophyll index (NDCI) (Mishra and Mishra, 2012).

$$2B = \frac{R_{705}}{R_{665}} \tag{1}$$

$$3B = \left(\frac{1}{R_{665}} - \frac{1}{R_{705}}\right) R_{740} \tag{2}$$

$$NDCI = \frac{R_{705} - R_{665}}{R_{705} + R_{665}} \tag{3}$$

As the matchup dataset was relatively small, we assessed the algorithm performance using existing calibrations from the literature instead of deriving site-specific coefficients for each of the Chl-*a* algorithms. A list of the calibrations used for Chl-*a* estimations, their references, and the range over which they were parameterized are shown in Table 2 and includes three different calibrations for the 2-band algorithm, two for the 3-band algorithm, and three for the NDCI.

Statistical metrics

Standard statistical metrics were used to determine the performance of each model output from the combination of the AC and Chl-*a* algorithm compared to the *in situ* Chl-*a* concentration. The metrics included the number of matchups (N), coefficient of determination (R^2), root-mean-square difference (RMSD), average absolute percentage difference (RPD), mean absolute difference (MAD) and the bias, expressed as follows:

$$RMSD = \sqrt{\frac{1}{N}\sum_{i=1}^{N}\left(\log_{10}\mathrm{Chl}_{mod} - \log_{10}\mathrm{Chl}_{meas}\right)^2} \tag{4}$$

$$RPD = \frac{1}{N}\sum_{i=1}^{N}\frac{\left|\mathrm{Chl}_{mod} - \mathrm{Chl}_{meas}\right|}{\mathrm{Chl}_{meas}} \times 100 \tag{5}$$

$$MAD = \frac{1}{N}\sum_{i=1}^{N}\left|\log_{10}\mathrm{Chl}_{mod} - \log_{10}\mathrm{Chl}_{meas}\right| \tag{6}$$

$$Bias = \frac{1}{N}\sum_{i=1}^{N}\left(\log_{10}\mathrm{Chl}_{mod} - \log_{10}\mathrm{Chl}_{meas}\right) \times 100 \tag{7}$$

where: Chl_{mod} is the algorithm-derived Chl-*a* output and Chl_{meas} is the *in situ* Chl-*a*. Since the distribution of Chl-*a* in the aquatic environment is log-normal (Campbell, 1995), the estimation of RMSD, MAD, bias and R^2 were performed on logarithmically transformed data. The significance of the correlation between *in situ* and satellite-derived Chl-*a* was evaluated using a Pearson correlation coefficient and a 2-tailed *t*-test. The null hypothesis (H_0: no correlation) was rejected if $p < 0.05$. Calculations were performed in Python (SciPy v1.10.1; Virtanen et al., 2020) using the *pearsonr* function, which accounts for sample size and correlation strength.

The performance of the combined AC and Chl-*a* algorithms was evaluated by Ogashawara et al. (2021), using a quantitative scoring system to rank their performance relative to the average statistical performance. Points were assigned based on standard deviation. For the RMSD, MAD, RPD and bias statistics, a score of 2, 1, or 0 was awarded where the algorithm statistic was within 1, 2 or more standard deviations of zero, respectively. For R^2, where the desired result was as close to 1 as possible, a score of 2, 1 or 0 was awarded when the algorithm statistic was within 1, 2 or more standard deviations of 1, respectively. For the *N* statistics, a score of 2, 1, or 0 was awarded if the total was within 1, 2 or more standard deviations of the maximum number of matchups, respectively.

Table 2. The algorithms used for Chl-*a* concentration retrieval from Sentinel-2 MSI data, showing the algorithm acronym, the equation with coefficients, the reference publication, and the Chl-*a* range over which the parameterisation was developed

Algorithm	Equation	Reference	Chl-*a* range (mg/m^3)
GL2B	$(35.745(2B) - 19.295)^{1.124}$	Gilerson et al. (2010)	0–80
GR2B	$25.28(2B)^2 + 14.85(2B) + 15.18$	Gurlin et al. (2011)	2.3–200.8
MS2B	$61.324(2B) - 37.94$	Moses et al. (2009)	0–70
GR3B	$315.50(3B)^2 + 215.95(3B) + 25.66$	Gurlin et al. (2011)	2.3–200.8
MS3B	$232.329(3B) + 23.174$	Moses et al. (2009)	0–70
M1ND	$314.97(NCDI)^2 + 236.5(NCDI) + 42.197$	Mishra and Mishra (2012)	0–30
M2ND	$194.325(NCDI)^2 + 86.115(NCDI) + 14.039$	Mishra and Mishra (2012)	0–30
MCND	$762.6(NCDI)^2 + 207.4(NCDI) + 16.4$	Maciel et al. (2023)	0.4–180

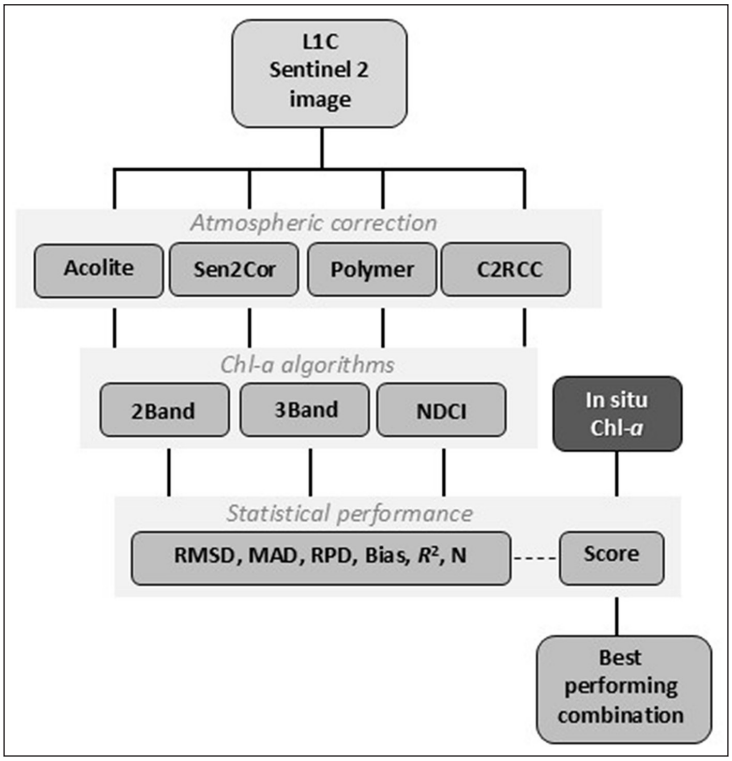

Figure 2. A diagram of satellite data processing and algorithm application

A total of 12 points could be scored, where the highest score represents the best-performing combination of algorithms. A flow diagram outlining all methods from Sentinel-2 download to final algorithm selection is provided in Fig. 2.

RESULTS AND DISCUSSION

AC and Chl-*a* algorithm performance

Although the current study is limited in its ability to comment on AC performance due to the lack of *in situ* radiometric measurements, this limitation is shared with many parts of the world. It should not be a prohibitive factor in evaluating the application of remote sensing data in under-represented areas. Several studies have even suggested that detecting Chl-*a* concentration in more eutrophic conditions is less affected by the selected AC product (Grendaité and Stonevičius, 2022; Matthews and Odermatt, 2015). As in Grendaité and Stonevičius (2022), the current study aims to comment on the performance of the combined output of the AC and the existing Chl-*a* algorithms in terms of applicability for water quality monitoring. Chegoonian et al. (2023) found that a combined assessment provided useful information regarding the desired application, e.g., improved accuracy or temporal stability. Pahlevan et al. (2021) also noted that globally there is no single solution for inland and coastal waters. AC processors should be selected according to the scientific objective or application.

The remote sensing reflectance (R_{rs}) outputs of the four AC schemes for several matchup stations are provided in Fig. 3, whereas the statistical performance of each of the 32 AC and Chl-*a* algorithm combinations are provided in Table 3. Overall, the C2RCC has a relatively flat spectral shape and slight variation in peaks and troughs, whereas only the magnitude of the entire reflectance spectrum changes between dates and stations. All Chl-*a* algorithms applied resulted in a generally negative bias, elevated RMSD (>0.812), low R^2 (<0.1) and no significant correlations ($p > 0.05$) (Table 3). Ansper and Alikas (2018) found that the C2RCC did not show good sensitivity in reproducing the absorption signal of Chl-*a* at 665 nm, which may explain the flat spectral shape and poor statistical performance for the C2RCC compared to the other AC algorithms.

Overall, Acolite showed the lowest scores and the least valid retrievals, and outputs were not available for all the matchups, possibly due to stringent default non-water masking settings that remove top-of-atmosphere data when the radiance at 1 600 nm is greater than 0.0215. Where Acolite reflectance is produced, it generally has a spectral shape and magnitude like that of Sen2Cor and is elevated in the visible range compared to C2RCC and Polymer; Sent et al. (2021) had similar findings for the Sado Estuary in Portugal where Acolite also over-estimated the R_{rs} compared to C2RCC and Polymer. Pereira-Sandoval et al. (2019) found that the performance of Sen2Cor and Acolite, in terms of statistical matchups with *in situ* reflectance, showed a relatively consistent mean absolute error and positive bias across the spectral range. However, that statistical performance improved over more eutrophic inland water types.

Although the magnitude for Sen2Cor is consistently elevated compared to the other ACs, it has a very similar spectral shape to that of Polymer in the red to near-infrared spectral range where *in situ* Chl-*a* was >30 mg/m^3 (Fig. 3b, c, d and f). In these cases the 705 nm reflectance peak, an important feature for Chl-*a* estimation in optically complex and eutrophic waters, is evident for both Sen2Cor and Polymer. Warren et al. (2019) further found that outputs from Sen2Cor had a lower spectral angle (i.e., more similar spectral shape to *in situ* reflectance) than Polymer over European inland waters. Studies have shown that although Sen2Cor performs poorly in coastal and marine waters, it tends to provide results comparable to other AC methods in inland waters (Warren et al., 2019; Grendaité and Stonevičius, 2022).

The best three combinations of AC-Chl algorithms, each with a score of 7, resulted from a combination of the NDCI algorithm with either Sen2Cor using the coefficients of Maciel et al. (2023) (MCND from Table 2) or with Sen2Cor and Polymer using the coefficients of Mishra and Mishra (2012) (M2ND from Table 2).

Table 3. The statistical performance of each AC and Chl-*a* algorithm (Chl-*a* Algo) combination, including the root-mean-squared-difference (RMSD), mean absolute difference (MAD), average absolute percent difference (RPD), bias, R^2, and number of positive modelled results (*N*) used for comparing modelled Chl-*a* (from algorithms applied to satellite reflectance) to *in situ* Chl-*a*, and the performance score. The three best-performing algorithms are indicated with *. Results that did not have a significant correlation ($p > 0.05$) are shown in italics.

AC	Chl-*a* Algo	RMSD	MAD	RPD (%)	Bias (%)	R^2	*p*-value	*N*	Score
*Sen2Cor	MCND	0.448	0.356	173.3	23.8	0.728	3.01×10^{-8}	26	7
Polymer	MCND	0.61	0.409	290	12.4	0.545	2.79×10^{-7}	36	6
ACOLITE	MCND	0.477	0.377	211.8	35	0.65	0.0016	12	4
C2RCC	*MCND*	*1.036*	*0.841*	*100.6*	*−65.9*	*0.08*	*0.1060*	*34*	*5*
Sen2Cor	M1ND	0.697	0.574	469.8	49.4	0.757	7.84×10^{-9}	26	4
Polymer	M1ND	0.707	0.509	477.5	20.3	0.436	1.19×10^{-5}	36	4
ACOLITE	M1ND	0.847	0.774	698.8	77.4	0.67	0.0011	12	1
C2RCC	*M1ND*	*0.948*	*0.793*	*386.7*	*−3.7*	*0.095*	*0.0759*	*34*	*5*
*Sen2Cor	M2ND	0.468	0.394	137.9	5.1	0.781	2.14×10^{-9}	26	7
*Polymer	M2ND	0.564	0.399	171.7	−8.8	0.603	2.59×10^{-8}	36	7
ACOLITE	M2ND	0.455	0.388	185.6	31.7	0.709	0.0006	12	5
C2RCC	*M2ND*	*0.969*	*0.778*	*136.5*	*−46.1*	*0.015*	*0.4932*	*34*	*5*
Sen2Cor	GL2B	0.548	0.463	240.6	23.1	0.767	4.72×10^{-9}	26	6
Polymer	GL2B	0.618	0.44	259.5	4.2	0.511	9.86×10^{-7}	36	6
ACOLITE	GL2B	0.63	0.548	355	52.3	0.693	0.0008	12	3
C2RCC	*GL2B*	*0.957*	*0.777*	*228.5*	*−25*	*0.094*	*0.0772*	*34*	*5*
Sen2Cor	GR2B	0.787	0.646	645.8	55.7	0.758	7.43×10^{-9}	26	4
Polymer	GR2B	0.826	0.7	787.5	56.4	0.526	5.67×10^{-7}	36	4
ACOLITE	GR2B	0.999	0.911	1069.6	91.1	0.755	0.0002	12	2
C2RCC	*GR2B*	*0.892*	*0.783*	*715.8*	*28.9*	*0.045*	*0.2291*	*34*	*4*
Sen2Cor	MS2B	0.546	0.462	239.6	23	0.751	1.05×10^{-8}	26	6
Polymer	MS2B	0.607	0.434	261	2.4	0.524	1.30×10^{-6}	34	6
ACOLITE	MS2B	0.621	0.537	346.4	51.4	0.663	0.0013	12	3
C2RCC	*MS2B*	*0.812*	*0.683*	*217*	*−15.1*	*0.003*	*0.7781*	*32*	*6*
Sen2Cor	GR3B	0.583	0.481	308.9	42.7	0.721	4.15×10^{-8}	26	5
Polymer	GR3B	0.611	0.461	437	33.3	0.691	6.16×10^{-10}	35	5
ACOLITE	GR3B	0.681	0.603	412.1	50.5	0.516	0.008476	12	3
C2RCC	*GR3B*	*0.887*	*0.751*	*252.5*	*−17.6*	*0.067*	*0.140414*	*34*	*5*
Sen2Cor	MS3B	0.539	0.425	256.2	33.6	0.703	1.68×10^{-7}	25	5
Polymer	MS3B	0.511	0.34	348.5	16.8	0.685	9.14×10^{-9}	31	6
ACOLITE	MS3B	0.619	0.499	357	34.8	0.479	0.0183	11	3
C2RCC	*MS3B*	*0.831*	*0.687*	*194.1*	*−20.7*	*0*	*0.9880*	*32*	*6*

Chawla et al. (2020) noted that the NDCI is superior to the 2B and 3B algorithms in turbid productive waters, while Makwinja et al. (2023) found that a quadratic function for NDCI, applied to Sen2Cor reflectance, produced satisfactory performance for mapping Chl-*a* of Lake Malombe, Malawi. To choose the best-performing combination of these three, the scatter plots and statistics over the entire *in situ* Chl-*a* range, as well as over Chl-*a* measurements exceeding 10 mg/m^3, are shown in Fig. 4. Although the combination of Sen2Cor and M2ND produced a smaller RPD and bias than the other combinations throughout the entire range of *in situ* Chl-*a* concentrations, the combination of Sen2Cor and MCND was closer to the 1:1 line when the *in situ* Chl-*a* concentrations were elevated, with a more negligible bias, RMSD, and MAD than the other two combinations. This makes it potentially more appropriate to monitor eutrophication. The Sen2Cor-MCND combination was selected for all subsequent calculations.

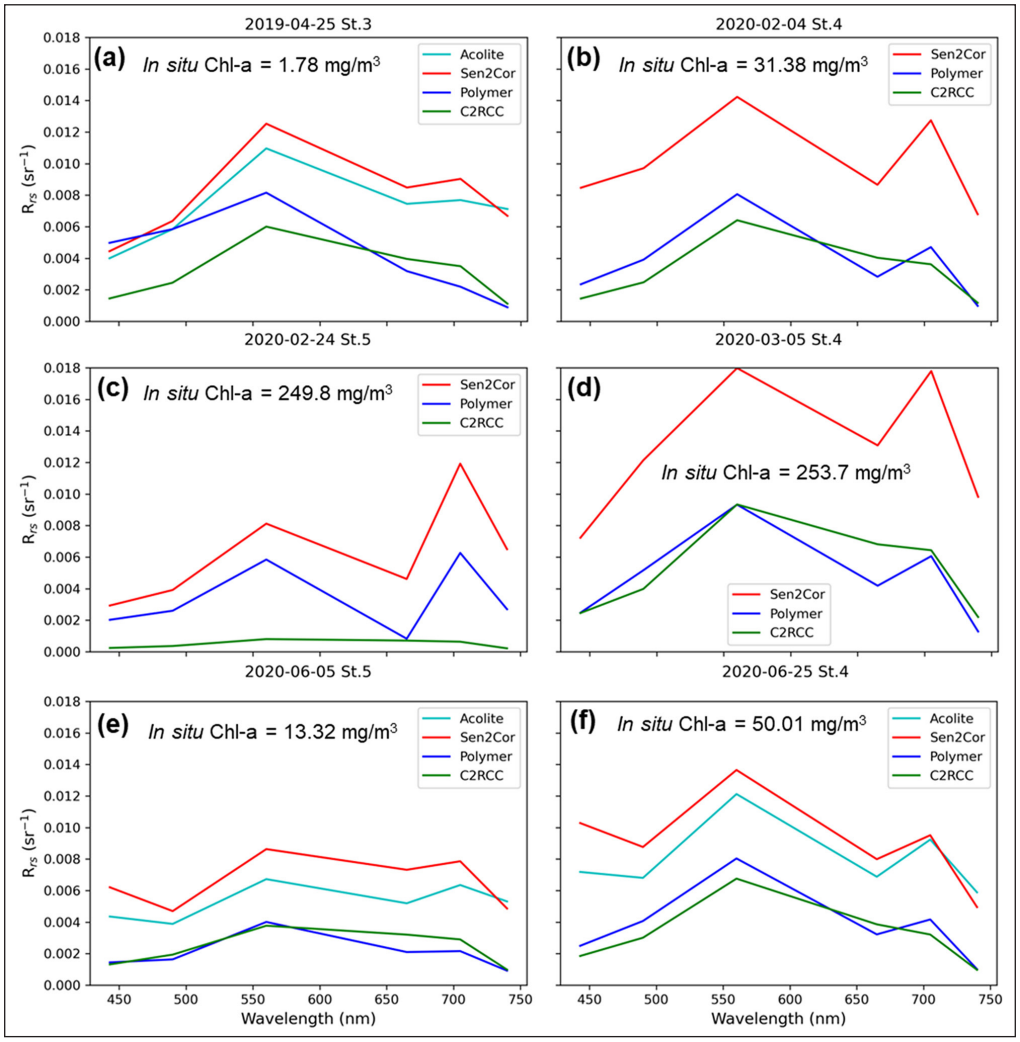

Figure 3. R_{rs} spectra of extracted matchup pixels showing outputs from the different ACs at a selection of stations in the Swartkops Estuary

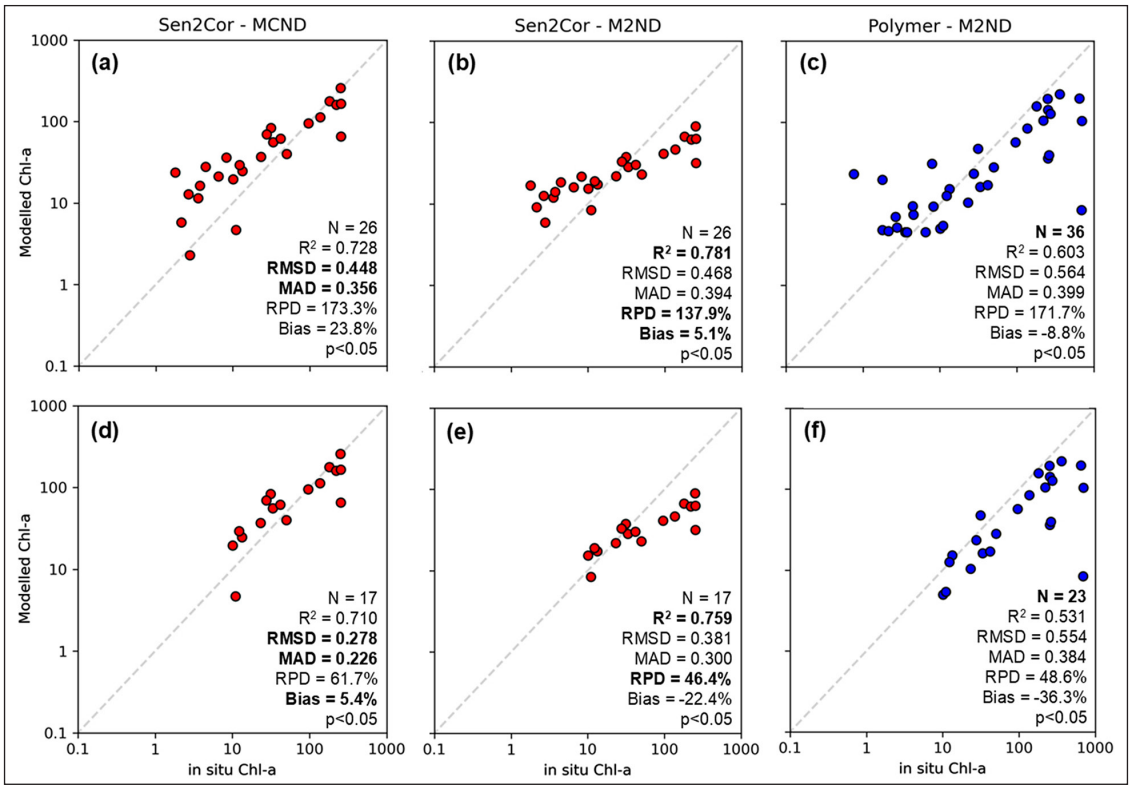

Figure 4. Scatterplots of the best-performing AC and Chl-*a* algorithm combinations (from Table 2). Panels a–c show all the available data, whereas panels d–f show only the data and statistics where *in situ* Chl-*a* >10 mg/m³

Regarding uncertainties for Chl-*a* retrievals

Several factors might contribute to the increase in the uncertainty of satellite-derived products. Although *in situ* measurements are often considered to represent the 'truth', standard methods for the determination of Chl-*a*, such as the fluorometric method, can have uncertainties of over 30% (Trees et al., 1985). There is also a spatial mismatch between the use of point-based measurements to represent an entire basin of a water body compared to the depth and spatial integration approach of satellite measurements (Papenfus et al., 2020). While the time window between field sampling and satellite data collection could affect the uncertainty, it should not be an issue in this study, as ± 3h aligns with recommendations for river systems (Kuhn et al., 2019) and is at the lower end of most matchup windows (Llodrà-Llabrés et al., 2023), which can range up to 12 days (Li et al., 2021). Uncertainties are expected to be greater in inland waters compared to coastal and oceanic environments (Pahlevan et al., 2021). For example, uncertainties ranged from approximately 10–1 400% for 70 AC and Chl-*a* algorithm combinations when applied to Sentinel-2 MSI data over Lithuanian lakes (Grendaité and Stonevičius, 2022).

Product uncertainty is also elevated in areas affected by adjacency effects (AE) (Warren et al., 2021), when the relatively greater reflectance from neighbouring land pixels influences those of the darker water pixels, which becomes apparent at wavelengths > 700 nm; however, studies found that AE may have a more minor impact when aquatic Chl-*a* concentrations are relatively high and if the water target is surrounded by green vegetation (Bulgarelli and Zibordi, 2018; Ruescas et al., 2016). In the current study, Sen2Cor and Acolite overestimated in the longer wavelengths compared to C2RCC and Polymer; Pereira-Sandoval et al. (2019) found that the reflectance at 740 and 783 nm for Sen2Cor and Acolite was higher than the *in situ* values, which they attributed to AE. It may be concluded that under increased AE conditions, the use of the 3-band algorithm (which includes longer wavelengths) might result in poorer performance and greater variations in performance between ACs.

This study supports the use of the NDCI coupled with Sen2Cor for monitoring eutrophication in the Swartkops Estuary – a methodology potentially transferable to similarly eutrophic estuaries surrounded by vegetation. It should be noted that, due to the dependence of Sen2Cor on the presence of dark vegetation for its correction, its accuracy could decrease in regions with less vegetation (Bui et al., 2022; Ruescas et al., 2016). Care should be taken in areas where the bottom of the estuary is visible, as these are likely to lead to an overestimation of satellite-derived Chl-*a* concentration. However, this is more likely to have an effect in the lower reaches of the estuary, where the water clarity is increased. The proposed algorithm combination has also shown poor performance at lower Chl-*a* concentration ranges. Future studies could consider using algorithm merging (e.g., Smith et al., 2018; Schaeffer et al., 2022) or applying an optical water-type approach, where the per-pixel spectral shape is considered and used to determine the most appropriate Chl-*a* algorithm or AC-Chl algorithm combination (e.g., Pahlevan et al., 2021; Soomets et al., 2020) to reduce uncertainties.

Implications for operational application and management opportunities

While high accuracy may be required for scientific studies, it is acknowledged that, typically, operational management could benefit from more qualitative metrics. Even with high uncertainty, concentration changes can be detected if the product is derived using a consistent methodology (Schaeffer et al., 2013). Several studies have pointed out the value of satellite-derived information even in the absence of accurate regressions between *in situ* and satellite data, particularly in terms of harmful algal bloom advisories, where a simple absence or presence information is desired (Schaeffer et al., 2018); similarly, categorical classification into trophic levels (Papenfus et al., 2020) can be helpful for water quality management purposes.

The selected AC-Chl algorithm combination was applied to a time series of Sentinel-2 reflectance on the Digital Earth Africa platform. Satellite-derived Chl-*a* concentrations were extracted at each station between April 2019 and October 2021, corresponding to the period represented by the *in situ* Chl-*a* dataset from Lemley et al. (2023). Figure 5 compares the *in situ* and satellite-derived concentrations for each station. The distributions are remarkably similar in terms of median values and concentration ranges, considering the varied temporal scales represented by the two datasets. Satellite data is rarely available for Station 6, as water hyacinth (*Pontederia crassipes*) frequently obscures the surface (Lakane et al., 2024). However, the spatial variations over most of the estuary are routinely captured by satellite data.

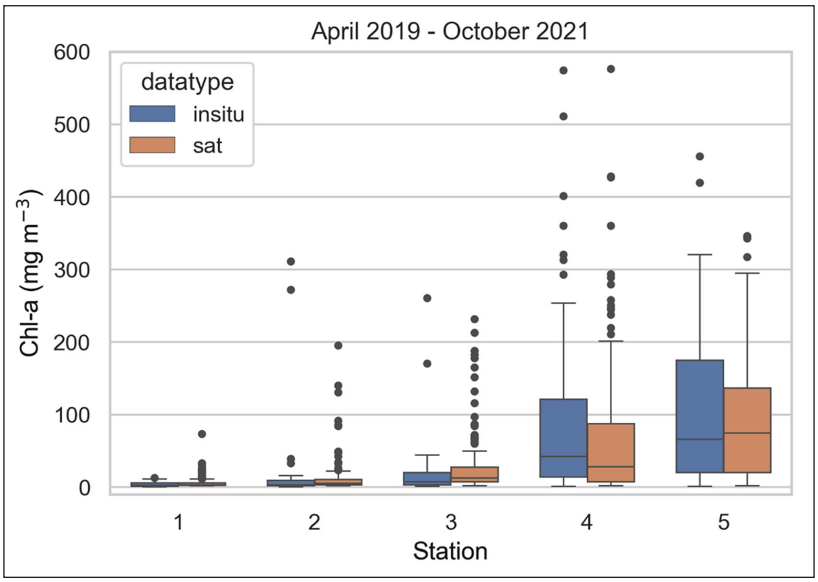

Figure 5. Boxplots for Stations 1 to 5 showing the Chl-*a* concentrations measured *in situ* and derived via satellite throughout the study. Note that the satellite product shows all available data over the study period (i.e. not only the matchup data).

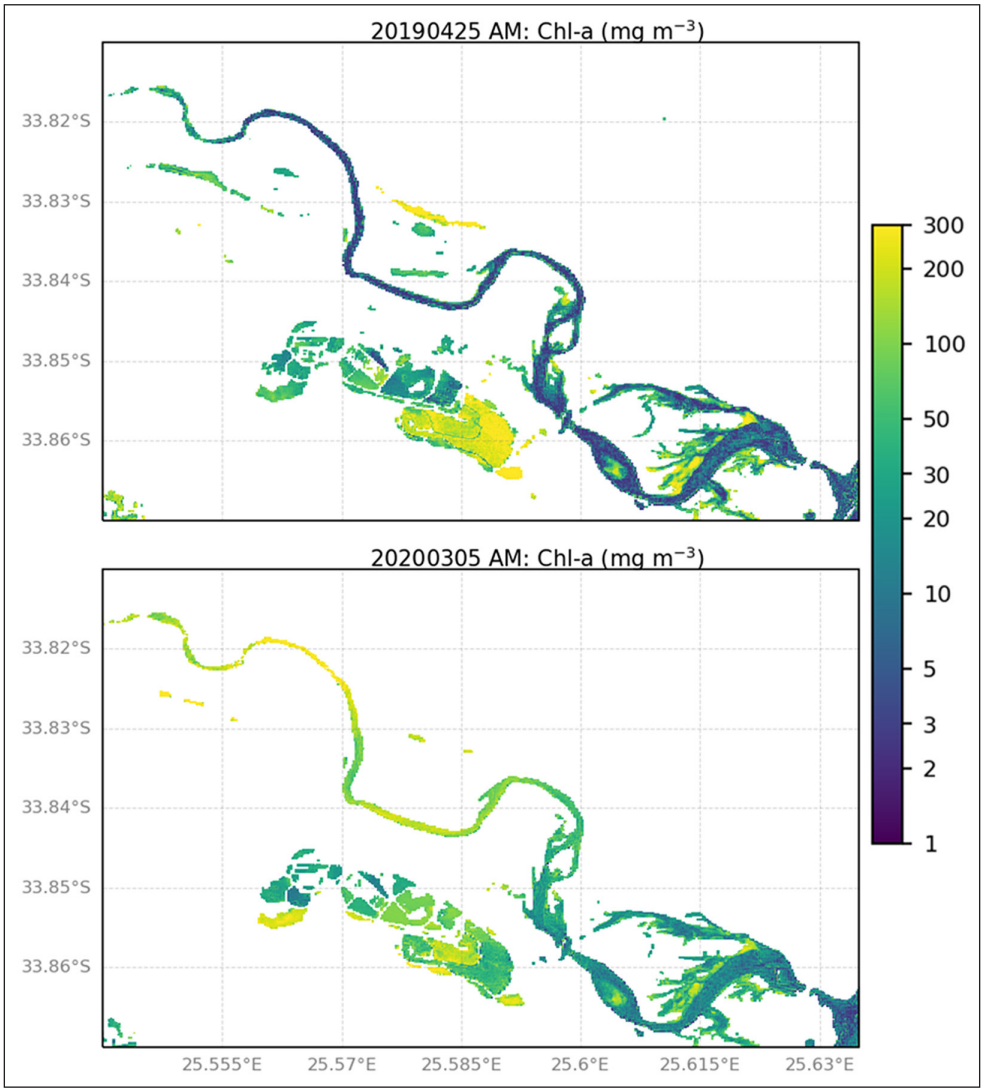

Figure 6. Examples of the Chl-*a* maps produced by applying the MCND (Maciel et al., 2023) to Standard L2 (Sen2Cor) Sentinel-2 MSI images. The 25 April 2019 and 5 March 2020 images correspond with generally low and elevated *in situ* Chl-*a* concentration ranges, respectively.

To evaluate the performance of the algorithms on the event scale, we produced maps of the Chl-*a* concentration for 25 April 2019 and 5 March 2020 (Fig. 6). On 25 April 2019, the *in situ* surface Chl-*a* ranged between 1.8 and 6.5 mg/m^3 from Stations 1 to 5, respectively, and reached 45.58 mg/m^3 at Station 6, while on 5 March 2020, the surface Chl-*a* concentrations at Stations 4 and 5 were approximately 253 mg/m^3. These ranges, seasonal variations, and spatial distributions are reproduced in the estuarine regions of Fig. 6. The Sen2Cor-NDCI combination has been used successfully for monitoring eutrophication in African and Brazilian reservoirs (Makwinja et al., 2023; Watanabe et al., 2019), strengthening the case for its applicability in eutrophic systems, such as the Hartenbos (Lemley et al., 2021) and Sundays (Lemley et al., 2018) estuaries in South Africa, to name just a few.

CONCLUSIONS

The results of our study indicate that, when used with appropriately configured empirical algorithms, the default Level-2A surface reflectance from Sentinel-2 can be used for water quality applications over mesotrophic and eutrophic estuaries; these findings are relevant to monitoring and water quality management of similarly sized estuaries globally. Care should be taken when applying this approach over oligotrophic water bodies, as the uncertainties and bias of the satellite-derived outputs tend to increase at *in situ* Chl-*a* concentrations < 10 mg/m^3. The satellite data used in the study are freely available on Cloud-based computational platforms such as Google Earth Engine and Digital Earth Africa, facilitating algorithm application, spatiotemporal scalability, and time-series analysis over the entire Sentinel-2 catalogue from 2017 to the present. The methodology in this study has been operationally implemented within the OCIMS Water Quality Decision Support Service (OCIMS, 2025), facilitating free, routine, and timely distribution of mapped Chl-*a* and derived products, which could be used to inform targeted *in situ* monitoring efforts and complement existing water quality monitoring and management by providing a holistic overview of a system.

ACKNOWLEDGEMENTS

The authors would like to thank: the NRF and SANSA NEO Frontiers programme (UID:142435) for funding; ESA for Sentinel-2 data; Digital Earth Africa for the use of their Sandbox processing platform; the Department of Forestry, Fisheries and Environment (DFFE) and Department of Science and Innovation (DSI) for funding through the OCIMS project; the South African Water Research Commission (WRC Project: C2020/2021–00076), a Communities of Practice grant from the NRF (GUN: 110612), and the DSI/NRF Research Chair in Shallow Water Ecosystems (UID: 84375) for financial support; the Zwartkops Conservancy for logistical support; and SAEON Elwandle node for logistical assistance in the field and laboratory through the SMCRI programme.

AUTHOR CONTRIBUTIONS

Marié E Smith: conceptualization, original draft preparation, validation, formal analysis, visualization. Daniel A Lemley: conceptualization, data curation, formal analysis, investigation, resources, writing – review and editing. Emily Whitfield: investigation, formal analysis, writing – review and editing. Janine B Adams: funding acquisition, resources, project administration, supervision, validation, writing – review and editing.

ORCIDS

Marié E Smith
https://orcid.org/0000-0001-6781-2343

Daniel A Lemley
https://orcid.org/0000-0003-0325-8499

Emily Whitfield
https://orcid.org/0000-0002-6900-8823

Janine B Adams
https://orcid.org/0000-0001-7204-123X

REFERENCES

ADAMS J, PRETORIUS L and SNOW G (2019) Deterioration in the water quality of an urbanised estuary with recommendations for improvement. *Water SA* **45** 86–96. https://doi.org/10.4314/wsa.v45i1.10

ADAMS JB, TSIPA V, VAN NIEKERK L, JAMES NC, LAMBERTH SJ, MADIKIZELA B, RIDDIN T, RISHWORTH GM, SNOW GC, STRYDOM NA, TALJAARD S and LEMLEY DA (2025) Health assessment and restoration options for the degraded Swartkops Estuary, South Africa. *Water SA* **51** (2) 90–106. https://doi.org/10.17159/wsa/2025.v51.i2.4142

ANSPER A and ALIKAS K (2018) Retrieval of chlorophyll *a* from Sentinel-2 MSI data for the European Union water framework directive reporting purposes. *Remote Sens.* **11** 64. https://doi.org/10.3390/rs11010064

BANGIRA T, MATONGERA TN, MABHAUDHI T and MUTANGA O (2023) Remote sensing-based water quality monitoring in African reservoirs, potential and limitations of sensors and algorithms: A systematic review. *Phys. Chem. Earth A/B/C* **134** 103536. https://doi.org/10.1016/j.pce.2023.103536

BROCKMANN C, DOERFFER R, PETERS M, KERSTIN S, EMBACHER S and RUESCAS A (2016) Evolution of the C2RCC neural network for Sentinel 2 and 3 for the retrieval of ocean colour products in normal and extreme optically complex waters. In: *Proceedings of the Living Planet Symposium*, 9–13 May 2016, Prague, Czech Republic.

BUI QT, JAMET C, VANTREPOTTE V, MÉRIAUX X, CAUVIN A and MOGRANE MA (2022) Evaluation of Sentinel-2/MSI atmospheric correction algorithms over two contrasted French coastal waters. *Remote Sens.* **14**. https://doi.org/10.3390/rs14051099

BULGARELLI B and ZIBORDI G (2018) On the detectability of adjacency effects in ocean color remote sensing of mid-latitude coastal environments by Sea-WiFS, MODIS-A, MERIS, OLCI, OLI and MSI. *Remote Sens. Environ.* **209** 423–438. https://doi.org/10.1016/j.rse.2017.12.021

CAMPBELL JW (1995) The lognormal distribution as a model for bio-optical variability in the sea. *J. Geophys. Res.: Oceans* (1978–2012) **100** 13237–13254. https://doi.org/10.1029/95JC00458

CHAWLA I, KARTHIKEYAN L and MISHRA AK (2020) A review of remote sensing applications for water security: Quantity, quality, and extremes. *J. Hydrol.* **585** 124826. https://doi.org/10.1016/j.jhydrol.2020.124826

CHEGOONIAN AM, PAHLEVAN N, ZOLFAGHARI K, LEAVITT PR, DAVIES JM, BAULCH HM and DUGUAY CR (2023) Comparative analysis of empirical and machine learning models for Chl *a* extraction using Sentinel-2 and Landsat OLI data: opportunities, limitations, and challenges. *Can. J. Remote Sens.* **49** 2215333. https://doi.org/10.1080/07038992.2023.2215333

COPERNICUS OPEN ACCESS HUB (2023) URL: https://scihub.copernicus.eu/ (Accessed 12 May 2023).

DALL'OLMO G, GITELSON AA and RUNDQUIST DC (2003) Towards a unified approach for remote estimation of chlorophyll-*a* in both terrestrial vegetation and turbid productive waters. *Geophys. Res. Lett.* **30**. https://doi.org/10.1029/2003GL018065

DIGITAL EARTH AFRICA (2024) DE Africa Analysis Sandbox. URL: https://docs.digitalearthafrica.org/en/latest/sandbox/index.html (accessed on 18 January 2024).

FRANZ BA, BAILEY SW, KURING N and WERDELL PJ (2015) Ocean color measurements with the Operational Land Imager on Landsat-8: implementation and evaluation in SeaDAS. *J. Appl. Remote Sens.* **9** 096070–096070. https://doi.org/10.1117/1.JRS.9.096070

GILERSON AA, GITELSON AA, ZHOU J, GURLIN D, MOSES W, IOANNOU I and AHMED SA (2010) Algorithms for remote estimation of chlorophyll-*a* in coastal and inland waters using red and near infrared bands. *Optics Express* **18** 24109–24125. https://doi.org/10.1364/OE.18.024109

GITELSON A and KONDRATYEV KY (1991) Optical models of mesotrophic and eutrophic water bodies. *Int. J. Remote Sens.* **12** 373–385. https://doi.org/10.1080/01431169108929659

IOCCG (2018) Earth observations in support of global water quality monitoring. In: Greb S, Dekker A, and Binding C (eds) *IOCCG Report Series, No. 20*, International Ocean Colour Coordinating Group, Dartmouth, Canada. https://doi.org/10.25607/OBP-1042

GRENDAITÉ D and STONEVIČIUS E (2022) Uncertainty of atmospheric correction algorithms for chlorophyll *a* concentration retrieval in lakes from Sentinel-2 data. *Geocarto Int.* **37** 6867–6891. https://doi.org/10.1080/10106049.2021.1958014

GURLIN D, GITELSON AA and MOSES WJ (2011) Remote estimation of chl-*a* concentration in turbid productive waters – return to a simple two-band NIR-red model? *Remote Sens. Environ.* **115** 3479–3490. https://doi.org/10.1016/j.rse.2011.08.011

KAUFMAN YJ, WALD AE, REMER LA, GAO BC, LI RR and FLYNN L (1997) The MODIS 2.1-/spl mu/m channel-correlation with visible reflectance for use in remote sensing of aerosol. *IEEE Trans. Geosci. Remote Sens.* **35** 1286–1298. https://doi.org/10.1109/36.628795

KRUG M, NAIDOO A and WILLIAMS L (2024) South Africa's oceans and coastal and information management system towards improved ocean access, protection, and governance. *J. Environ. Manage.* **354** 120255. https://doi.org/10.1016/j.jenvman.2024.120255

KUHN C, DE MATOS VALERIO A, WARD N, LOKEN L, SAWAKUCHI HO, KAMPEL M, RICHEY J, STADLER P, CRAWFORD J, STRIEGL R, VERMOTE E, PAHLEVAN N and BUTMAN D (2019) Performance of Landsat-8 and Sentinel-2 surface reflectance products for river remote sensing retrievals of chlorophyll-a and turbidity. *Remote Sens. Environ.* **224** 104–118. https://doi.org/10.1016/j.rse.2019.01.023

LAKANE CP, ADAMS JB and LEMLEY DA (2024) Drivers of seasonal water hyacinth dynamics in permanently eutrophic estuarine waters. *Biol. Invasions* **26** 2831–2849. https://doi.org/10.1007/s10530-024-03347-w

LEMLEY DA, ADAMS JB and STRYDOM NA (2018) Triggers of phytoplankton bloom dynamics in permanently eutrophic waters of a South African estuary. *Afr. J. Aquat. Sci.* **43** 229–240. https://doi.org/10.2989/16085914.2018.1478794

LEMLEY DA, HUMAN LR, RISHWORTH GM, WHITFIELD E and ADAMS JB (2023) Managing the seemingly unmanageable: Water quality and phytoplankton dynamics in a heavily urbanised low-inflow estuary. *Estuar. Coasts* **46** 2007–2022. https://doi.org/10.1007/s12237-022-01128-z

LEMLEY DA, LAKANE CP, TALJAARD S and ADAMS JB (2022) Inorganic nutrient removal efficiency of a constructed wetland before discharging into an urban eutrophic estuary. *Mar. Pollut. Bull.* **179** 113727. https://doi.org/10.1016/j.marpolbul.2022.113727

LEMLEY DA, LAMBERTH SJ, MANUEL W, NUNES M, RISHWORTH GM, VAN NIEKERK L and ADAMS JB (2021) Effective management of closed hypereutrophic estuaries requires catchment-scale interventions. *Front. Mar. Sci.* **8** 688933. https://doi.org/10.3389/fmars.2021.688933

LI S, SONG K, WANG S, LIU G, WEN Z, SHANG Y, LYU L, CHEN F, XU S, TAO H and co-authors (2021) Quantification of chlorophyll-*a* in typical lakes across China using Sentinel-2 MSI imagery with machine learning algorithm. *Sci. Tot. Environ.* **778** 146271. https://doi.org/10.1016/j.scitotenv.2021.146271

LLODRÀ-LLABRÉS J, MARTÍNEZ-LÓPEZ J, POSTMA T, PÉREZ-MARTÍNEZ C and ALCARAZ-SEGURA D (2023) Retrieving water chlorophyll-*a* concentration in inland waters from Sentinel-2 imagery: Review of operability, performance and ways forward. *Int. J. Appl. Earth Observ. Geoinf.* **125** 103605. https://doi.org/10.1016/j.jag.2023.103605

MACIEL FP, HAAKONSSON S, PONCE DE LEÓN L, BONILLA S and PEDOCCHI F (2023) Challenges for chlorophyll-*a* remote sensing in a highly variable turbidity estuary, an implementation with Sentinel-2. *Geocarto Int.* **38** 2160017. https://doi.org/10.1080/10106049.2022.2160017

MAIN-KNORN M, PFLUG B, LOUIS J, DEBAECKER V, MÜLLER-WILM U and GASCON F (2017) Sen2Cor for Sentinel-2. In: *Image and Signal Processing for Remote Sensing XXIII*, 26–29 September 2016, Edinburgh, Scotland.

MAKWINJA R, INAGAKI Y, SAGAWA T, OBUBU JP, HABINEZA E and HAAZIYU W (2023) Monitoring trophic status using *in situ* data and Sentinel-2 MSI algorithm: Lesson from Lake Malombe, Malawi. *Environ. Sci. Pollut. Res.* **30** 29755–29772. https://doi.org/10.1007/s11356-022-24288-8

MATTHEWS MW and ODERMATT D (2015) Improved algorithm for routine monitoring of cyanobacteria and eutrophication in inland and near-coastal waters. *Remote Sens. Environ.* **156** 374–382. https://doi.org/10.1016/j.rse.2014.10.010

MISHRA S and MISHRA DR (2012) Normalized difference chlorophyll index: A novel model for remote estimation of chlorophyll-*a* concentration in turbid productive waters. *Remote Sens. Environ.* **117** 394–406. https://doi.org/10.1016/j.rse.2011.10.016

MMACHAKA T, NEL MA, SNOW B and ADAMS JB (2023) Reduction in pollution load to an urban estuary using a sustainable drainage system treatment train. *Mar. Pollut. Bull.* **194** 115378. https://doi.org/10.1016/j.marpolbul.2023.115378

MOSES WJ, GITELSON AA, BERDNIKOV S and POVAZHNYY V (2009) Satellite estimation of chlorophyll-*a* concentration using the red and NIR bands of MERIS—the Azov sea case study. *IEEE Geosci. Remote Sens. Lett.* **6** 845–849. https//doi.org/10.1109/LGRS.2009.2026657

MÜLLER-WILM U, DEVIGNOT O and PESSIOT L (2018) Sen2Cor Configuration and User Manual. S2-PDGS-MPC-L2A-SUM-V2.5.5.2.

NDOU N (2023) Geostatistical inference of Sentinel-2 spectral reflectance patterns to water quality indicators in the Setumo dam, South Africa. *Remote Sens. Appl.: Soc. Environ.* **30** 100945. https://doi.org/10.1016/j.rsase.2023.100945

NUSCH EA (1980) Comparison of different methods for chlorophyll and phaeopigment determination. *Arch. Hydrobiol. Beih. Ergebn. Limnol.* **14** 14–36.

OBAID A, ALI K, ABIYE T and ADAM E (2021) Assessing the utility of using current generation high-resolution satellites (Sentinel 2 and Landsat 8) to monitor large water supply dam in South Africa. *Remote Sens. Appl.: Soc. Environ.* **22** 100521. https://doi.org/10.1016/j.rsase.2021.100521

OCIMS (2025) The OCIMS Water Quality Decision Support Tool. URL: https://ocims.csir.co.za/water-quality/#/viewer/new (Accessed 21 May 2025).

OGASHAWARA I, KIEL C, JECHOW A, KOHNERT K, RUHTZ T, GROSSART HP, HÖLKER F, NEJSTGAARD JC, BERGER SA and WOLLRAB S (2021) The use of Sentinel-2 for spatial dynamics assessment: A comparative study on different lakes in northern Germany. *Remote Sens.* **13** 1542. https://doi.org/10.3390/rs13081542

PAHLEVAN N, MANGIN A, BALASUBRAMANIAN SV, SMITH B, ALIKAS K, ARAI K, BARBOSA C, BÉLANGER S, BINDING C, BRESCIANI M and co-authors (2021) ACIX-Aqua: A global assessment of atmospheric correction methods for Landsat-8 and Sentinel-2 over lakes, rivers, and coastal waters. *Remote Sens. Environ.* **258** 112366. https://doi.org/10.1016/j.rse.2021.112366

PAHLEVAN N, SARKAR S, FRANZ B, BALASUBRAMANIAN S and HE J (2017) Sentinel-2 MultiSpectral Instrument (MSI) data processing for aquatic science applications: Demonstrations and validations. *Remote Sens. Environ.* **201** 47–56. https://doi.org/10.1016/j.rse.2017.08.033

PAPENFUS M, SCHAEFFER B, POLLARD AI and LOFTIN K (2020) Exploring the potential value of satellite remote sensing to monitor chlorophyll-*a* for US lakes and reservoirs. *Environ. Monit. Assess.* **192** 808. https://doi.org/10.1007/s10661-020-08631-5

PEREIRA-SANDOVAL M, RUESCAS A, URREGO P, RUIZ-VERDÚ A, DELEGIDO J, TENJO C, SORIA-PERPINYÀ X, VICENTE E, SORIA J and MORENO J (2019) Evaluation of atmospheric correction algorithms over Spanish inland waters for Sentinel-2 multi spectral imagery data. *Remote Sens.* **11** 1469. https://doi.org/10.3390/rs11121469

RUESCAS A, PEREIRA-SANDOVAL M, TENJO C, RUIZ-VERDÚ A, STEINMETZ F and DE KEUKELAERE L (2016) Sentinel-2 atmospheric correction intercomparison over two lakes in Spain and Peru-Bolivia. In: *Proceedings of the Colour and Light in the Ocean from Earth Observation (CLEO) Workshop*, Frascati, Italy.

SCHAEFFER BA, SALLS W, COFFER M, LEBRETON C, WERTHER M, STELZER K, URQUHART E and GURLIN D (2022) Merging of the Case 2 Regional Coast Colour and Maximum-Peak Height chlorophyll-*a* algorithms: validation and demonstration of satellite-derived retrievals across US lakes. *Environ. Monit. Assess.* **194** 179. https://doi.org/10.1007/s10661-021-09684-w

SCHAEFFER BA, BAILEY SW, CONMY RN, GALVIN M, IGNATIUS AR, JOHNSTON JM, KEITH DJ, LUNETTA RS, PARMAR R, STUMPF RP and URQUHART EA (2018) Mobile device application for monitoring cyanobacteria harmful algal blooms using Sentinel-3 satellite Ocean and Land Colour Instruments. *Environ. Model. Softw.* **109** 93–103. https://doi.org/10.1016/j.envsoft.2018.08.015

SCHAEFFER BA, SCHAEFFER KG, KEITH D, LUNETTA RS, CONMY R and GOULD RW (2013) Barriers to adopting satellite remote sensing for water quality management. *Int. J. Remote Sens.* **34** (21) 7534–7544. https://doi.org/10.1080/01431161.2013.823524

SENT G, BIGUINO B, FAVARETO L, CRUZ J, SÁ C, DOGLIOTTI AI, PALMA C, BROTAS V and BRITO AC (2021) Deriving water quality parameters using sentinel-2 imagery: A case study in the Sado Estuary, Portugal. *Remote Sens.* **13** 1–30. https://doi.org/10.3390/rs13051043

SMITH ME, LAIN LR and BERNARD S (2018) An optimized chlorophyll *a* switching algorithm for MERIS and OLCI in phytoplankton-dominated waters. *Remote Sens. Environ.* **215** 217–227. https://doi.org/10.1016/j.rse.2018.06.002

SOOMETS T, UUDEBERG K, JAKOVELS D, BRAUNS A, ZAGARS M and KUTSERT (2020) Validation and comparison of water quality products in Baltic lakes using Sentinel-2 MSI and Sentinel-3 OLCI data. *Sensors* **20** 742. https://doi.org/10.3390/s20030742

TREES CC, KENNICUTT II MC and BROOKS JM (1985) Errors associated with the standard fluorimetric determination of chlorophylls and phaeopigments. *Mar. Chem.* **17** 1–12. https://doi.org/10.1016/0304-4203(85)90032-5

STEINMETZ F, DESCHAMPS P-Y and RAMON D (2011) Atmospheric correction in presence of sun glint: application to MERIS. *Optics Express* **19** 9783–9800. https://doi.org/10.1364/OE.19.009783

STEINMETZ F and RAMON D (2018) Sentinel-2 MSI and Sentinel-3 OLCI consistent ocean colour products using polymer. In: *Remote Sensing of the Open and Coastal Ocean and Inland Waters*, 24-25 September 2018, Honolulu, Hawaii, USA.

VANHELLEMONT Q (2019) Adaptation of the dark spectrum fitting atmospheric correction for aquatic applications of the Landsat and Sentinel-2 archives. *Remote Sens. Environ.* **225** 175–192. https://doi.org/10.1016/j.rse.2019.03.010

VANHELLEMONT Q and RUDDICK K (2015) Advantages of high quality SWIR bands for ocean colour processing: Examples from Landsat-8. *Remote Sens. Environ.* **161** 89–106. https://doi.org/10.1016/j.rse.2015.02.007

VANHELLEMONT Q and RUDDICK K (2018) Atmospheric correction of metre-scale optical satellite data for inland and coastal water applications. *Remote Sens. Environ.* **216** 586–597. https://doi.org/10.1016/j.rse.2018.07.015

VIRTANEN P, GOMMERS R, OLIPHANT TE, HABERLAND M, REDDY T, COURNAPEAU D, BUROVSKI E, PETERSON P, WECKESSER W, BRIGHT J and co-authors (2020) SciPy 1.0: fundamental algorithms for scientific computing in Python. *Nat. Meth.* **17** (3) 261–272. https://doi.org/10.1038/s41592-019-0686-2

WARREN MA, SIMIS SG, MARTINEZ-VICENTE V, POSER K, BRESCIANI M, ALIKAS K, SPYRAKOS E, GIARDINO C and ANSPER A (2019) Assessment of atmospheric correction algorithms for the Sentinel-2A MultiSpectral Imager over coastal and inland waters. *Remote Sens. Environ.* **225** 267–289. https://doi.org/10.1016/j.rse.2019.03.018

WARREN MA, SIMIS SG and SELMES N (2021) Complementary water quality observations from high and medium resolution Sentinel sensors by aligning chlorophyll-*a* and turbidity algorithms. *Remote Sens. Environ.* **265** 112651. https://doi.org/10.1016/j.rse.2021.112651

WATANABE F, ALCÂNTARA E, BERNARDO N, DE ANDRADE C, GOMES AC, DO CARMO A, RODRIGUES T and ROTTA LH (2019) Mapping the chlorophyll-*a* horizontal gradient in a cascading reservoirs system using MSI Sentinel-2A images. *Adv. Space Res.* **64** 581–590. https://doi.org/10.1016/j.asr.2019.04.035